ELSEVIER

Journal of Alloys and Compounds 311 (2000) 114–119

Journal of ALLOYS AND COMPOUNDS

www.elsevier.com/locate/jallcom

# The magnetic structure of $TbNiAlD_{1.1}$

H.W. Brinks[a], V.A. Yartys[a,*], B.C. Hauback[a], H. Fjellvåg[b], K. Yvon[c], F. Gingl[c,1], T. Vogt[d]

[a]*Institute for Energy Technology, P.O. Box 40, Kjeller N-2027, Norway*
[b]*Department of Chemistry, University of Oslo, P.O. Box 1033 Blindern, Oslo N-0315, Norway*
[c]*Laboratoire de Cristallographie, Université de Genève, 24 quai Ernest Ansermet, CH-1211 Genève 4, Switzerland*
[d]*Physics Department, Brookhaven National Laboratory, Upton, Long Island, NY 11973, USA*

Received 27 April 2000; accepted 12 May 2000

**Abstract**

The magnetic structure of orthorhombic $TbNiAlD_{1.1}$ was determined by powder neutron diffraction at 3.8 and 10 K, below the antiferromagnetic ordering temperature $T_N=11$ K. The unit cell is doubled in **b** and **c** directions compared to the nuclear unit cell (space group *Amm*2; at 3.8 K $a=3.6554$; $b=12.3954$; $c=7.6316$ Å), and the magnetic moments are confined to the **bc** plane with main component along **c**. The magnetic structure is different from TbNiAl and $TbNiAlD_{0.3}$ which both have ordered magnetic moments along the corresponding **a** axis. The magnetic moments of Tb1 and Tb2 at 3.8 K are 6.8 and 5.7 $\mu_B$, respectively. On heating to 10 K, the type of magnetic structure is not changed, however, $\mu$(Tb) are decreased to 2.9 $\mu_B$ (Tb1) and 5.4 $\mu_B$ (Tb2). 

*Keywords:* Magnetic structure; Terbium nickel aluminium deuteride; Crystal structure; Metal hydride; Neutron diffraction

## 1. Introduction

TbNiAl has the ability to absorb up to 1.4 deuterium atoms per formula unit, and intermediate phases with 0.3, 0.8 and 1.1 D atoms have been isolated [1,2]. The first one retains the basic hexagonal metal sublattice of TbNiAl (space group $P\bar{6}2m$), whereas higher deuterium contents result in an orthorhombic distortion (space group *Amm*2); $\mathbf{a}=\mathbf{c}_{hex}$, $\mathbf{b}=2\mathbf{a}_{hex}+\mathbf{b}_{hex}$, $\mathbf{c}=\mathbf{b}_{hex}$ (unit-cell dimensions: $\sim c_{hex}$, $\sqrt{3}\ a_{hex}$, $a_{hex}$).

The magnetic ordering of the intermetallic TbNiAl phase has been described on the basis of powder [3] and single crystal [4] neutron diffraction studies. The ordering temperature of the Tb sublattice is $T_N=47$ K [3]. Furthermore, there is a magnetic phase transition at $T_1=23$ K [3,4]. Symmetry analysis, obtained from the hexagonal nuclear symmetry and the observed propagation vector $\mathbf{k}=(\frac{1}{2}, 0, \frac{1}{2})$, reveals a splitting of the Tb site into two orbits which could order independently with $\mathbf{k}$, $\mathbf{k}'=(\frac{1}{2}, \frac{1}{2}, 0)$ or $\mathbf{k}''=(-\frac{1}{2}, \frac{1}{2}, \frac{1}{2})$ [4]. At 5 K, neutron diffraction experiments prove that 2/3 of the Tb atoms are ordered with propagation vector $\mathbf{k}$ and 1/3 with propagation vector $\mathbf{k}'$ or $\mathbf{k}''$, with equally large moments (~7.9 $\mu_B$) along $\mathbf{c}_{hex}$ [4]. Above 10 K, the moments of the latter sublattice decrease quickly relative to the former, and are ~1 $\mu_B$ above $T_1$ [3]. Between $T_1$ and $T_N$ both orbits have propagation vector $\mathbf{k}$ with moments along **c** [4].

Rather sparse data are available for the magnetic properties of TbNiAl-deuterides or hydrides. Powder neutron diffraction (PND) studies at 7 and 28 K have shown that $TbNiAlD_{0.3}$ takes the high-temperature magnetic structure of TbNiAl [2]. $TbNiAlH_{0.7}$ has approximately the same magnetic ordering temperature as TbNiAl [5]. In $TbNiAlD_{0.8}$, studied as a two-phase mixture, reflections of magnetic origin are observed in the PND pattern below 20 K, and they can partially be indexed on a unit cell with doubling of the orthorhombic **a** and **b** axes [6]. For $TbNiAlD_{1.28}$, two magnetic reflections at $d=7.21$ and 12.90 Å are present in the PND pattern below 16 K [6]. For $TbNiAlH_{1.4}$, $T_N=14.5$ K was established [5].

The present study provides the first description of the magnetic structure of an orthorhombic ZrNiAl-type deuteride. The presently obtained results for $TbNiAlD_{1.1}$

*Corresponding author. Tel.: +47-63-80-6453; fax: +47-63-81-0920.
*E-mail address:* volodymyr.yartys@ife.no (V.A. Yartys).
[1]Current address: Energy Conversion Devices, Inc., 1675 West Maple Road, Troy, MI 48084, USA.

0925-8388/00/$ – see front matter 
PII: S0925-8388(00)01034-3

are discussed in relation to magnetic properties for the hexagonal analogues, TbNiAl and $TbNiAlD_{0.3}$.

## 2. Experimental

The $TbNiAlD_{1.1}$ sample was identical to the one studied in Ref. [1] and was achieved by ageing of saturated $TbNiAlD_{1.4}$. TbNiAl was prepared from Tb (purity 99.8%), Ni (99.9%) and Al (99.9%) by arc melting in an argon atmosphere. The ingots were remelted several times to increase their homogeneity. X-ray powder diffraction (Philips PW 1012/10 and Huber–Guinier diffractometers, CuKα radiation) confirmed the presence of TbNiAl with ZrNiAl-type crystal structure [$a=6.999(1)$ and $c=3.879(2)$ Å] plus traces of an unidentified impurity phase. After activation in vacuum at 300°C, deuteration was performed at room temperature and ambient pressure.

Powder neutron diffraction data of $TbNiAlD_{1.1}$ were collected at 3.8 and 10 K with the High-Resolution Neutron Powder Diffractometer [7] at the High-Flux Beam Reactor, Brookhaven National Laboratory. Experimental details: focusing Ge(511) monochromator, $\lambda=1.8857$ Å, $2\theta_{max}=155°$, $\Delta 2\theta=0.05°$, sample mass 7 g, cylindrical vanadium container of 9 mm diameter and cryostate temperature controller.

The program Fullprof [8] was used for Rietveld refinements. Scattering lengths and magnetic form factor for $Tb^{3+}$ were taken from the program library.

Magnetic susceptibility was measured in a field of 500 G by a Magnetic Property Measurement System, Quantum Design (with SQUID sensor). The zero-field cooled sample was kept as a free powder in a gelatin capsule. Calibration was carried out by means of a Pd standard (from NIST). The studied sample was prepared by desorption of a fresh $TbNiAlD_{1.4}$ sample in vacuum at 293 K.

Table 1
Crystallographic and magnetic structure parameters of $TbNiAlD_{1.1}$ from Rietveld refinements of high-resolution PND data ($\lambda$ 1.8857 Å)[a]

| | 3.8 K | 10 K | 293 K |
|---|---|---|---|
| $a$/Å | 3.6554(1) | 3.6565(1) | 3.7019(1) |
| $b$/Å | 12.3954(2) | 12.3951(3) | 12.4011(3) |
| $c$/Å | 7.6316(2) | 7.6288(2) | 7.6075(2) |
| $V$/Å$^3$ | 345.79 | 345.76 | 349.24 |
| $y$(Tb1) | – | 0.2117(4) | 0.2092(4) |
| $z$(Tb1) | – | 0.040(2) | 0.031(2) |
| $z$(Tb2) | – | 0.646(3) | 0.639(2) |
| $y$(Ni1) | – | 0.3294(3) | 0.3319(3) |
| $z$(Ni1) | – | 0.274(3) | 0.261(2) |
| $z$(Ni2) | – | 0.247(3) | 0.236(2) |
| $y$(Al1) | – | 0.1166(11) | 0.1181(8) |
| $z$(Al1) | – | 0.330(3) | 0.323(2) |
| $z$(Al2) | – | 0.0000(-) | 0.0000(-) |
| $y$(D1) | – | 0.3329(6) | 0.3343(5) |
| $z$(D1) | – | 0.270(3) | 0.251(2) |
| $y$(D2) | – | 0.3783(8) | 0.3821(6) |
| $z$(D2) | – | 0.084(3) | 0.067(2) |
| $y$(D3) | – | 0.2414(-) | 0.2414(10) |
| $z$(D3) | – | 0.402(-) | 0.402(3) |
| $B_{Tb1}$/Å$^2$ | – | 0.1(1) | 1.1(1) |
| $B_{Tb2}$/Å$^2$ | – | 1.7(2) | 1.2(2) |
| $B_{Ni1}$/Å$^2$ | – | 0.7(1) | 1.4(1) |
| $B_{Ni2}$/Å$^2$ | – | 0.9(1) | 1.8(1) |
| $B_{Al1}$/Å$^2$ | – | 1.4(2) | 1.0(2) |
| $B_{Al2}$/Å$^2$ | – | 2.2(4) | 2.1(3) |
| $B_D$/Å$^2$ | – | 1.2(1) | 2.2(1) |
| $\mu_y$(Tb1)/$\mu_B$ | 1.8(2) | 0.75(5) | – |
| $\mu_z$(Tb1)/$\mu_B$ | 6.7(6) | 2.76(5) | – |
| $\mu$(Tb1)/$\mu_B$ | 6.9(6) | 2.9(2) | – |
| $\mu_y$(Tb2)/$\mu_B$ | 3.9(4) | 3.82(14) | – |
| $\mu_z$(Tb2)/$\mu_B$ | 4.1(4) | 3.82(14) | – |
| $\mu$(Tb2)/$\mu_B$ | 5.6(6) | 5.4(2) | – |
| $R_p$/% | 5.87 | 5.54 | 4.1 |
| $\chi^2$ | 8.52 | 2.54 | 1.38 |
| $R_B$/% | 7.15 | 11.6 | |
| $R_M$/% | 10.5 | 24.1 | – |

[a] Space group *Amm*2 (#38): Tb1 in 4*e* ($\frac{1}{2}$, *y*, *z*), Tb2 in 2*b* ($\frac{1}{2}$, 0, *z*), Ni1 in 4*d* (0, *y*, *z*), Ni2 in 2*b*, Al1 in 4*d*, Al2 in 2*a* (0, 0, *z*), D1 in 4*e*, D2 in 4*d*, D3 in 4*d*. Deuterium occupation numbers are constrained to the values at 293 K taken from Ref. [1]: $n$(D1)=0.877, $n$(D2)=0.674 and $n$(D3)=0.10. Calculated standard deviations in parentheses.

## 3. Results

By cooling from 293 to 5 K, the unit-cell volume decreases by 0.99%, corresponding to an average linear thermal-expansion coefficient $\alpha_V=3.4\cdot10^{-5}$ K$^{-1}$ (Table 1). The volume reduction is anisotropic, with an increase of the *c* axis and negligible reduction of *b*. This anomalous variation is probably caused by magnetostriction with the onset of long-range magnetic ordering (main direction of the magnetic moments is [001], with a smaller component along [*010*], vide infra).

Some relatively weak additional peaks of magnetic origin are present in the PND diagram at 10 K (Fig. 1). On further cooling to 3.8 K, large magnetic intensity contributions are observed for scattering angles up to $2\theta\approx70°$. This suggests an ordering temperature slightly above 10 K. The magnetic peaks at 10 K are significantly broader than the nuclear ones. This effect is less at 3.8 K. At both temperatures the low-angle magnetic peaks are asymmetric compared to the nuclear peaks.

There are no indications in the magnetic susceptibility data (Fig. 2) for any ferro/ferrimagnetic components. The maximum in the magnetic susceptibility at $T_N=11$ K corresponds to onset of antiferromagnetic order. Above this temperature, there is a shoulder in the susceptibility curve which may be caused by short-range ordering. Alternatively, there is a magnetic phase transition at 11 K between two different magnetic arrangements. Curie–Weiss law is fulfilled above 55 K ($\mu_p=9.289(5)$ $\mu_B$, $\theta_p=-1.7(2)$ K; compared to theoretical $\mu_p=9.72$ $\mu_B$ for $Tb^{3+}$).

On application of large magnetic fields up to 50 kOe, no field-induced transition occurs (figure not shown). Hence,

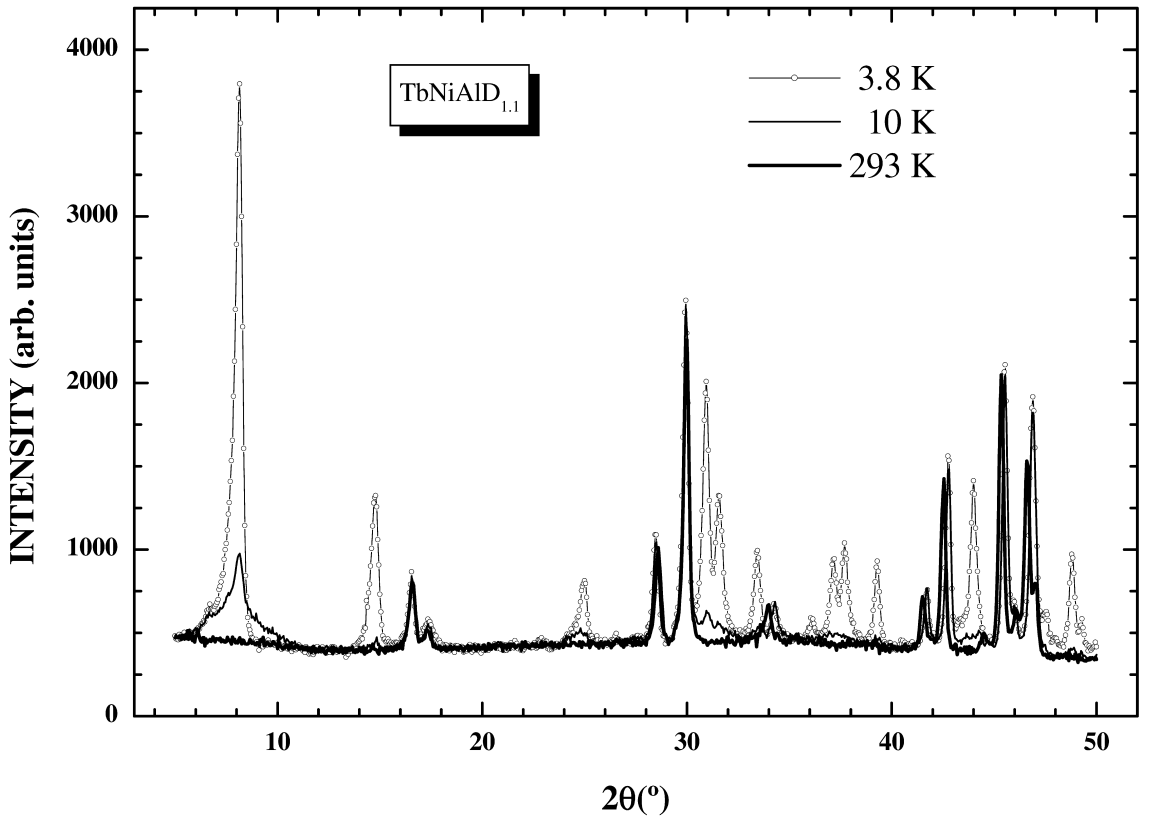


Fig. 1. Powder neutron diffraction data ($\lambda = 1.8857$ Å) of $TbNiAlD_{1.1}$ at 293 K (thick line), 10 K (thin line) and 3.8 K (line + circles) showing additional magnetic scattering contributions at low temperatures.

$TbNiAlD_{1.1}$ behaves differently from TbNiAl where a ferromagnetic state is induced for $H > 4$ kOe [4].

The magnetic reflections in the PND pattern at 3.8 K were indexed on a unit cell with doubled **b** and **c** axes relative to the nuclear structure. Examination of the systematic extinctions reveal A centering ($hkl$, $k+l=2n$), which is consistent with $\mathbf{k}=(0, \frac{1}{2}, \frac{1}{2})$. The choice of **k** is based on the assumption that the first magnetic peak is one single asymmetric peak with no contribution from the possible (001). As an alternative, the structure may be described by a primitive monoclinic unit cell with $\mathbf{a}_{mono} = \mathbf{c}_{ortho} + \mathbf{b}_{ortho}$, $\mathbf{b}_{mono} = \mathbf{a}_{ortho}$, $\mathbf{c}_{mono} = \mathbf{c}_{ortho} - \mathbf{b}_{ortho}$ and $\beta \approx 116.8°$ (see Fig. 3). This is a pseudohexagonal unit cell which is related to the unit cell of TbNiAl with doubled $a_{hex}$ and $b_{hex}$. Because of the data resolution, it was not possible to distinguish between the orthorhombic and monoclinic description, and the simpler orthorhombic model was preferred.

The magnetic unit cell contains 24 formula units. By means of the magnetic propagation vector the number of independent magnetic moments to be determined is reduced from 24 to 6. The relative positions of these six Tb atoms {Tb1 in 4*e* [Approximate positions: $Tb1_1$ ($\frac{1}{2}$, 0.10, 0), $Tb1_2$ ($\frac{1}{2}$, 0.15, 0.25), $Tb1_3$ ($\frac{1}{2}$, 0.35, 0.25), $Tb1_4$ ($\frac{1}{2}$, 0.40, 0)] and Tb2 in 2*b* [$Tb2_1$ ($\frac{1}{2}$, 0, 0.38), $Tb2_2$ ($\frac{1}{2}$, 0.25, 0.12)]} are illustrated in Fig. 3.

Since no symmetry analysis by representation theory is available, like e.g. the one carried out for TbNiAl with $\mathbf{k}=(\frac{1}{2}, 0, \frac{1}{2})$, the different possibilities for moment orientations were tested on a partial trial-and-error basis. On the basis of the observed strong magnetic reflections, e.g., (011), (111) and (071), the magnetic moments were assumed to be confined to the **bc** plane, with their main components along **c**. By refining different models with magnetic moments along **c**, covering all 16 combinations of signs for the six Tb atoms on the two Tb sublattices, one model proved significantly superior. The derived reliability factor was $R_p = 6.67\%$, compared to 9.3–9.9% for the other models. The Tb atoms of the superior model have the signs (+ means magnetic moment component along [001], whereas − means along [00$\bar{1}$]) $+-++$ for $Tb1_1, \ldots, Tb1_4$ and $-+$ for $Tb2_1$ and $Tb2_2$, hereafter abbreviated $(+-++,-+)$. The A-centered antiferromagnetic structure is shown in Fig. 3.

The reliability factor for the overall intensity profile $R_p$ was further reduced from 6.67% to 5.87% by introducing a magnetic component along **b**, whereas no improvements were achieved for components along **a**. Several combinations of the signs for the component along **b** gave rather similar quality of fit. The final model $(+---,++)$ was preferred by giving a significantly improved $R_{Mag}$ and has magnetic moments which are parallel or antiparallel for the

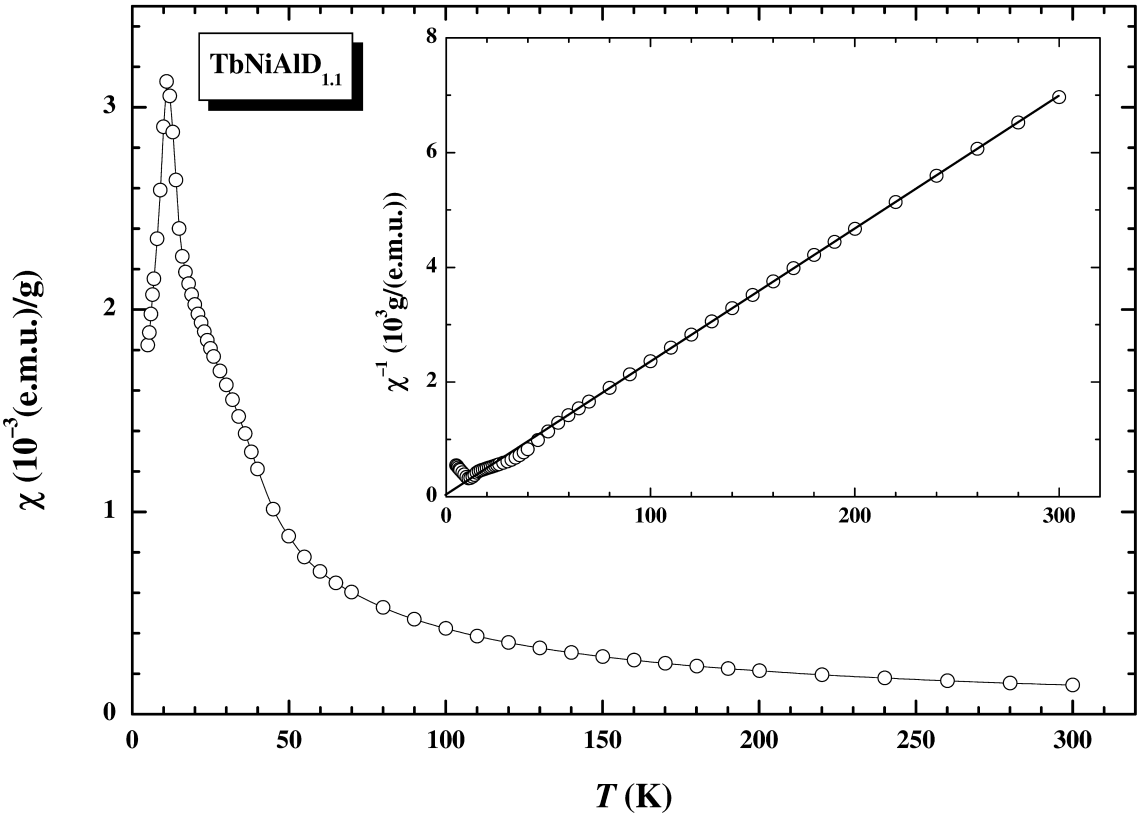


Fig. 2. Magnetic susceptibility of $TbNiAlD_{1.1}$ at 500 G below 300 K showing a maximum at 11 K. Inset: Inverse susceptibility of $TbNiAlD_{1.1}$ at 500 G.

Tb-atoms in each 'chain' ($Tb1_1$, $Tb1_2$ as well as $Tb1_3$, $Tb1_4$) and they point to a good approximation towards or opposite to that of one nearest Tb1 neighbor in the 'chain'. The refined magnetic moment is 6.8 $\mu_B$ for Tb1 ($\mu_z/\mu_y =$ 3.6) and 5.7 $\mu_B$ for Tb2 ($\mu_z/\mu_y = 1.0$).

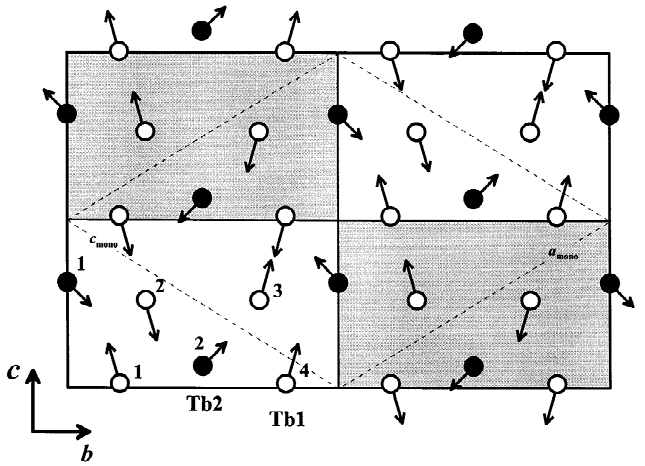


Fig. 3. Magnetic ordering of the Tb atoms in $TbNiAlD_{1.1}$ at 3.8 K, all Tb located in $x=\frac{1}{2}$. The numbering of magnetic atoms of the two non-equivalent Tb sublattices are shown. The A centering between the quadrants (nuclear unit cell) is illustrated by shading. Dashed lines show the alternative monoclinic unit cell. The Tb 'chains', from which the magnetic moments are rotated 15°, are running along [001].

The obtained structural and magnetic parameters from the refinements are given in Table 1, and the fit between observed and calculated intensity profiles is illustrated in Fig. 4.

The magnetic structure refinements assumed equally-sized magnetic moments for the Tb atoms corresponding to the two independent Tb sublattices. The possibility of further magnetic non-equivalence was tested by allowing free variation of the individual magnetic moments on all the six Tb atoms, however, this did not improve the fit.

The weaker magnetic Bragg scattering in the PND data at 10 K gives rise to peak shapes that hardly could be refined satisfactorily (Fig. 5). Nevertheless, refinements of these data, with the structural parameters and the direction of the magnetic moment constrained equal to the 3.8 K situation, show that the magnetic moment of Tb1 decreases significantly, whereas no major reduction is found for Tb2. This may indicate two different ordering temperatures for the two different Tb sublattices. However, no distinct indications are evident in the $\chi(T)$ data, see Fig. 2.

## 4. Discussion

The obtained data do not allow unequivocal determination of the **b** component of the magnetic moments. Different models, which in addition partly influence the

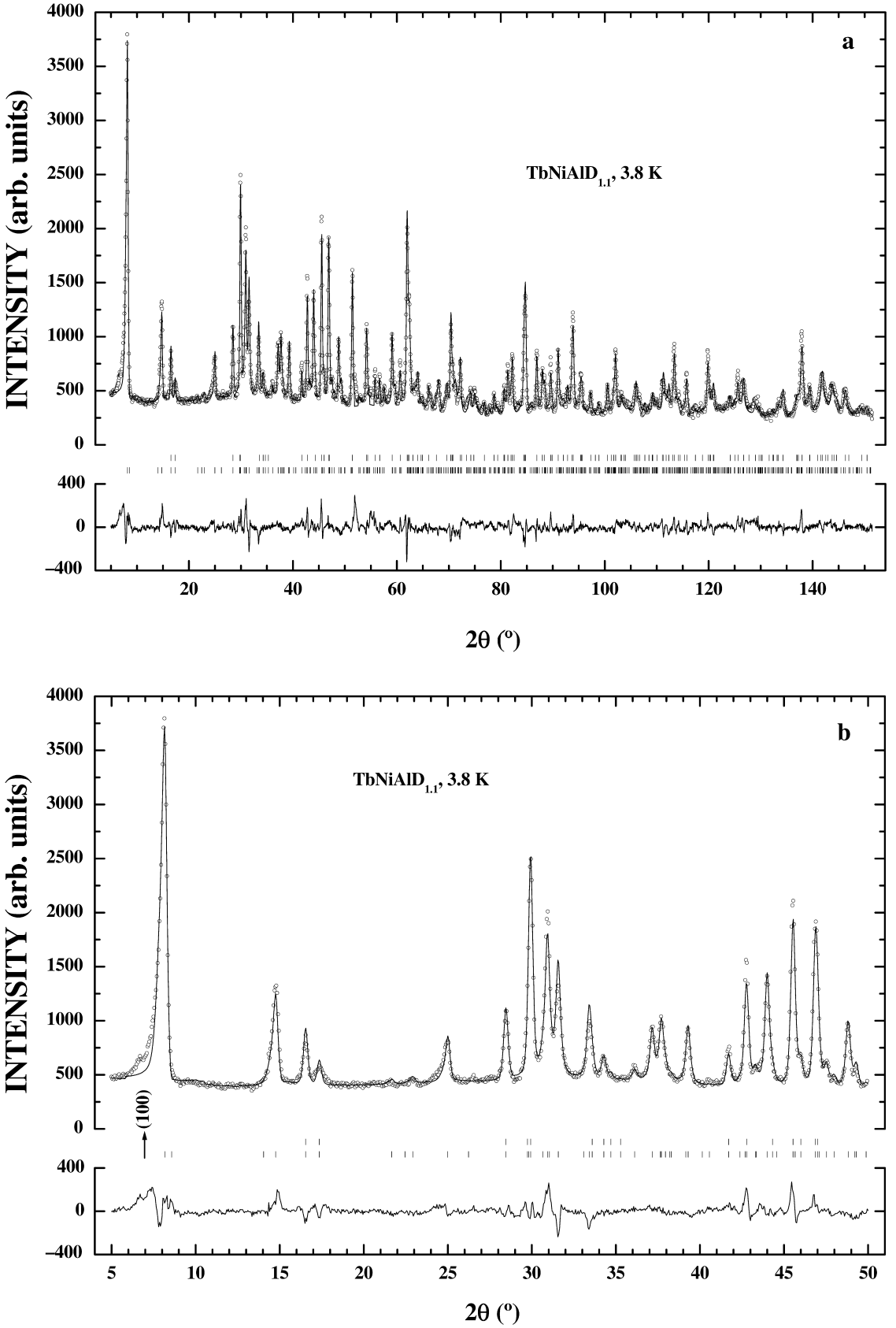


Fig. 4. Rietveld refinements (upper line) of PND data for $TbNiAlD_{1.1}$ at 3.8 K ($\lambda = 1.8857$ Å). (a) Full diagram, (b) low-angle part. Positions of Bragg reflections are shown with bars for the nuclear (upper) and magnetic (bottom) contributions. The lower curve shows the differences between observed and calculated intensities.

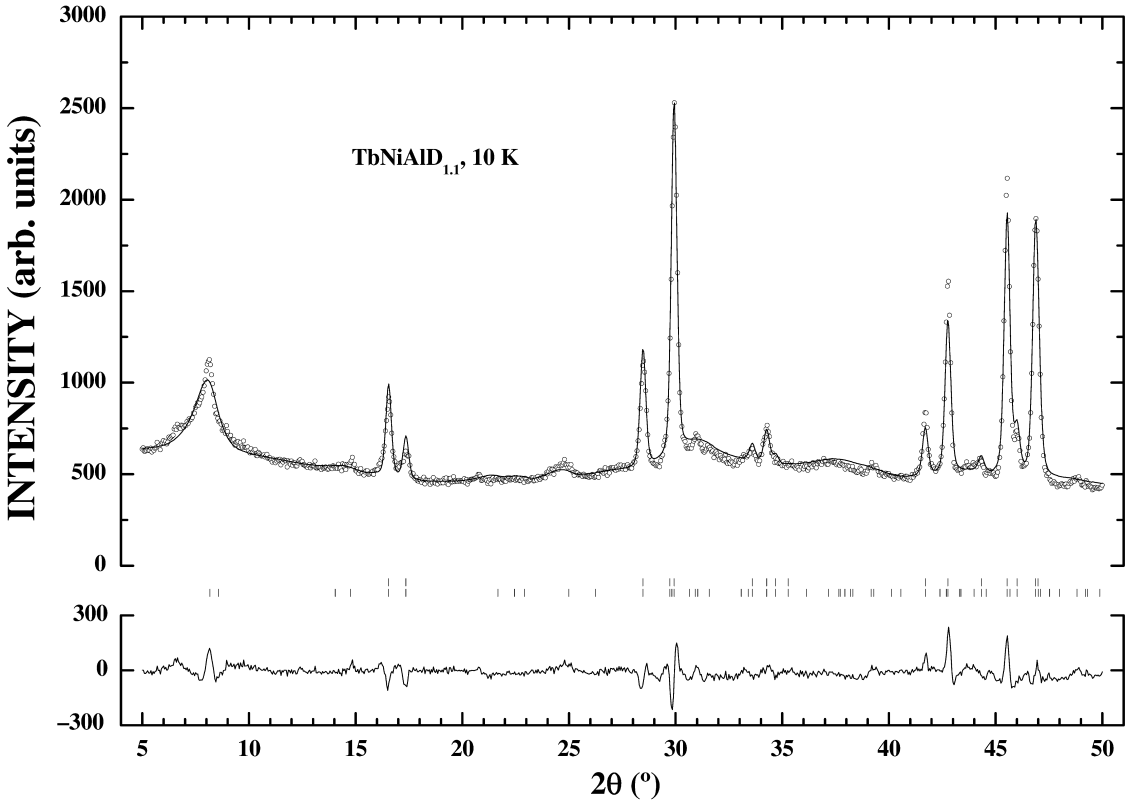


Fig. 5. Rietveld refinements (upper line) of low-angle PND data for $TbNiAlD_{1.1}$ at 10 K ($\lambda = 1.8857$ Å). Positions of Bragg reflections are shown with bars for the nuclear (upper) and magnetic (bottom) contributions. The lower curve shows the differences between observed and calculated intensities.

total magnetic moment of Tb1, give almost identical $R_p$, e.g. changing the sign of Tb2 from $++$ to $+-$ alters $R_p$ only from 5.87 to 5.90%, but affects the magnetic arrangement considerably. The model with the simplest plausible structure was selected. No other model shows better reliability factors.

In the PND study by Bordallo et al. [6], the strongest magnetic peaks were observed at similar *d*-spacings as presently. Their proposed magnetic unit cell, with doubling of **b** and **c** rather than doubling of **a** and **b**, is probably a result of improper setting of the orthorhombic space group. Hence, there is no contradiction between the present report and the observations by Bordallo et al. [6].

The deuteration of TbNiAl has two important effects that influences the magnetic interactions. First, the resulting anisotropic unit-cell expansion alters the Tb–Tb distances. RKKY interactions will be susceptible to subtle changes in the interatomic distances. Second, the incorporated deuterium atoms donate electrons to the electron structure which presumably is not strongly perturbed relatively to that of the intermetallic compound, although the symmetry is reduced from $P\bar{6}2m$ to $Amm2$. The sum of these effects evidently lowers the magnetic ordering temperature considerably, and the magnetic moment orientation changes from being parallel to the hexagonal axis (for TbNiAl) to become perpendicular. The latter effect is possibly caused by the anisotropic lattice expansion on deuteration.

## References

[1] V.A. Yartys, F. Gingl, K. Yvon, L.G. Akselrud, A.V. Kolomietz, L. Havela, T. Vogt, I.R. Harris, B.C. Hauback, J. Alloys Comp. 279 (1998) L4.
[2] B.C. Hauback, H. Fjellvåg, L. Pålhaugen, V.A. Yartys, K. Yvon, J. Alloys Comp. 295 (1999) 178.
[3] G. Ehlers, H. Maletta, Z. Phys. B 99 (1996) 145.
[4] P. Javorsky, P. Burlet, V. Sechovsky, A.V. Andreev, J. Brown, P. Svoboda, J. Magn. Magn. Mater. 166 (1997) 133.
[5] A.V. Kolomiets, L. Havela, V.A. Yartys, A.V. Andreev, J. Alloys Comp. 253 (1997) 343.
[6] H.N. Bordallo, H. Nakotte, J. Eckert, A.V. Kolomiets, L. Havela, A.V. Andreev, H. Drulis, W. Iwasieczko, J. Appl. Phys. 83 (1998) 6986.
[7] S.M. Shapiro, Neutron News 3 (1992) 7.
[8] J. Rodríguez-Carvajal, FULLPROF version 0.2, (LLB, Saclay, 1998).